bioRxiv preprint doi: https://doi.org/10.1101/2020.09.05.284208; this version posted September 6, 2020. The copyright holder for this preprint (which was not certified by peer review) is the author/funder. All rights reserved. No reuse allowed without permission.

Characterization of gustatory receptor 7 in the brown planthopper reveals functional versatility

Running title: *Nl*Gr7 reveals functional versatility

Abhishek Ojha, Wenqing Zhang □

State Key Laboratory of Biocontrol and School of Life Sciences, Sun Yat-sen University, Guangzhou, Guangdong 510275, China.

First author should be addressed; Abhishek Ojha, Email: abhishekitrc@rediffmail.com

□ Corresponding author should be addressed; Wenqing Zhang,

Email: lsszwq@mail.sysu.edu.cn, Tel: +862039332963; Fax: +862039943515.

Abstract

Insect pests consume tastants as their necessary energy and nutrient sources. Gustatory receptors play important roles in insect life and can form within an extremely complicated regulatory network. However, there are still many gustatory genes that have a significant impact on insect physiology, but their functional mechanism is still unknown. Here, we purified and characterized a gustatory receptor (protein) coding gene, *NlGr7*, from the brown planthopper (BPH) *Nilaparvata lugens*, which is an important insect pest of rice. Our results revealed that *Nl*Gr7 has an active association with various ligands, such as lectins, lipids (phospho- and sphingolipid) and copper. The mass-spectrometry result showed that *Nl*Gr7 is a sugar receptor, and *Nl*Gr7 is validated by different types of insoluble polysaccharides and a varied range of tastants. Furthermore, we observed that *Nl*Gr7-bound ATP hydrolysed on the ATPase activity assay, which indicated that *Nl*Gr7 may be associated with important biological functions in the BPH. The important *Nl*Gr7 for chemoreception has now been characterized in the BPH. We showed that *Nl*Gr7 in the BPH is required for various protein-ligands, as well as protein-sugars interactions, to play crucial roles in this pest. This study will provide valuable information for further functional studies of chemoreception mechanisms in this important agricultural pest.

Keywords: Sugar gustatory receptor, *Nilaparvata lugens*, Protein purification, Protein-ligands binding, ATP hydrolysis.

bioRxiv preprint doi: https://doi.org/10.1101/2020.09.05.284208; this version posted September 6, 2020. The copyright holder for this preprint (which was not certified by peer review) is the author/funder. All rights reserved. No reuse allowed without permission.

Introduction

Arthropods' gustatory receptors (Grs) are active in leading insect feeding behaviours and in establishing the platform between insect gustation and the environment. The Grs are closely associated with insect olfactory receptors (Ors) (**Robertson et al., 2003**). Grs have been investigated as divergent domains of seven-TM (transmembrane) spanning proteins, which is a typical example of G protein-coupled receptors (GPCRs), but they are noticeably diverse and impart no sequence resemblance with Grs of mammals (**Clyne et al., 2000)**. In addition, the topology of Gr' seven-TM helices are reversed in comparison to that of the GPCRs (**Zhang et al., 2011**). Although having well-established information on olfaction (**Benton et al., 2006; Robertson et al., 2006**) and increasing documentation of insect Grs, little known about the physiological mechanisms that include understanding of the gustation system.

The *Gr* genes were first established in *Drosophila* (**Clyne et al., 2000**), which is a polyphagous dipteran insect, and forty-three putative *Gr* genes have been revealed in this insect (**Amrein and Throne, 2005**). Grs have been documented into various clades and are named as sugar (**Slone et al., 2007)**, bitter (**Wanner and Robertson, 2008**; **Lee et al., 2009**), carbon dioxide (CO_2) (**Xu and Anderson, 2015**), GR43a-like (**Kui et al., 2018**), sex attractant (**Shankar et al., 2015**), and unknown (**Kui et al., 2018**) receptors, based on their sequence homologies with receptors that have been discovered in *Drosophila* (**Robertson et al., 2003**) or on an important molecule to which they reacted (**Kui et al., 2018**). Seventy-six and 79 *Gr* genes have been respectively identified in *Anopheles gambiae* (**Hill et al., 2002**) and *Aedes aegypti* (**Kent et al., 2008**), which is a hematophagous dipteran insect. Sixty-five and 197 *Gr* genes have been noted in the lepidopteran insects *Bombyx mori* (**Wanner and Robertson, 2008**) and *Helicoverpa armigera* (**Xu et al., 2016**), respectively. The highest number of *Gr* genes, 220, has been observed in *Tribolium castaneum*, which is a Coleopteran insect (**Richards et al., 2008**). Currently, the majority of research consideration has been focused on the *Gr* genes of *Drosophila* (**Slone et al., 2007; Dunipace et al., 2001; Gardiner et al., 2008; Weiss et al., 2011; Dahanukar et al., 2001; Dahanukar et al., 2007**); however, with fast-growing genome examinations on an additional species of insects (**Robertson and Wanner, 2006; Wanner and Robertson, 2008; Richards et al., 2008; Smadja et al., 2009; Xue et al., 2014**), the investigation is approaching a different spectrum of species. However, there is a need to shed light on the *Gr* genes in an important agricultural insect, such as the brown planthopper. The brown planthopper (BPH), *Nilaparvata lugens* (Stål) (Hemiptera: Delphacidae), is one of the most serious agricultural planthopper species and feeds on rice

bioRxiv preprint doi: https://doi.org/10.1101/2020.09.05.284208; this version posted September 6, 2020. The copyright holder for this preprint (which was not certified by peer review) is the author/funder. All rights reserved. No reuse allowed without permission.

plants (**Ojha and Zhang, 2019**). Recently, thirty-two putative *Gr* genes in this insect have been reported from our research group (**Kui et al., 2018**). However, the gustatory perception of these *Gr* genes, or the protein macromolecular platform, in the physiology of this insect has remained largely unknown.

In the present investigation, the functional properties of BPH Gr7 (*Nl*Gr7, protein) have been revealed after homologous expression in *E. coli*. Purified *Nl*Gr7 was examined for its association with lectins, lipids, polysaccharides, metals, and ATPase activity assays. These results are essential for understanding the molecular level of taste regulation within the BPH feeding behaviour and improve our understanding of the insect sugar-receptor family, insect-plant interaction and adaptation.

Materials and Methods

Insect sample

The BPH strain was maintained and reared on susceptible rice (Huang Hua Zhan) plants as described by Kui et al (2018).

Bioinformatics

The *Nl*Gr7 (protein) sequence was examined for different parameters, including the molecular weight, theoretical pI, amino acid composition, atomic composition, extinction coefficient, estimated half-life, instability index, aliphatic index and grand average of hydropathicity, by using an ExPASY ProtParam tool (https://web.expasy.org/protparam/). The TOPCONS tool was used to predict a secretory signal sequence and the transmembrane helix in the *Nl*Gr7 (http://topcons.cbr.su.se/). Furthermore, the *Nl*Gr7 sequence was searched with other known annotated insect Grs for sequence identity and to build a phylogenetic tree using protein BLAST tools from the NCBI weblink (https://www.ncbi.nlm.nih.gov/blast/treeview/treeView).

Cloning, expression, purification and biotin labelling of *Nl*Gr7

The total RNA of the female adult BPH was isolated by using a TRIzol reagent (Invitrogen, Carlsbad, CA), and one μg RNA was converted to cDNA by using the PrimeScript^{TM} RT-PCR Kit (Takara, Japan) following the manufacturer's instructions. Then, 10 ng cDNA was used as a template for PCR to amplify *NlGr7* using the forward primer 5'-CATATC-ATGTTGTTACTGACAATTGTTTTGATT-3' containing an *NdeI* sequence and the reverse primer 5'-GAATTC-TCACTGTGTTCTGCGCGTTT-3' containing an *EcoRI* sequence. A

bioRxiv preprint doi: https://doi.org/10.1101/2020.09.05.284208; this version posted September 6, 2020. The copyright holder for this preprint (which was not certified by peer review) is the author/funder. All rights reserved. No reuse allowed without permission.

PCR was carried out in 25 µl containing 200 µM dNTPs, 5 U *Taq* DNA polymerase (New England Biolabs, NEB, Inc, USA) and 13 µM of each of the primers. The PCR conditions were 95°C for 2 min, followed by 35 cycles at 95°C for 30 s, 55°C for 30 s, and 72°C for 30 s, with a final extension step at 72°C for 5 min. Amplicon (~730 bp) was analysed on 1% (w/v) agarose gel, was gel-purified using HiPure Gel Pure DNA Micro kit (Magen, China) following the manufacturer's instructions and was quantified using the NanoVue Plus spectrophotometer. The PCR product was digested with *NdeI* and *EcoRI* and was ligated to pMAL-c5X (NEB, Inc, USA). *Escherichia coli* (*E. coli*, DH5α) was used for transformation of the pMAL-c5X-*NlGr7* plasmid. The transformed bacteria were selected by screening the colonies on ampicillin (50 µg/ml) containing media and plasmid purification. Then, the colonies were further analysed by restriction enzyme digestion and PCR. The *NlGr7* gene of the recombinant plasmid was sequenced by the Sanger method. The expression host *E. coli* BL21(DE3)pLysS was used as a transformation host for the pMAL-c5X-*NlGr7* vector. A single colony of transformed *E. coli* BL21(DE3)pLysS with pMAL-c5X-*NlGr7* was incubated overnight in a shaking incubator in 500 ml Luria Bertani (LB) medium containing ampicillin (50 µg/ml) and chloramphenicol (34 µg/ml) at 37°C with constant agitation (200 rpm). The transformed cells at 25°C (OD_{600} = 0.6) were induced with 0.5 mM isopropyl b-D-thiogalactopyranoside (IPTG; Sigma, USA), which resulted in the expression of the maltose-binding protein (MBP)-tagged *Nl*Gr7 protein. After 8 h of induction, the cells were harvested at 5,0009xg for 15 min. The pellet was resuspended in a lysis buffer containing 50 mM Tris–HCl, pH 8.0, 200 mM NaCl, 3 mM β-ME, 10% v/v glycerol, and 0.15 mg/ml lysozyme. Cells were lysed by sonication (50 Hz, 20 cycles, with each cycle consisting of 20 s on- and 120 s off-time, 4°C), and the sonicated suspension was centrifuged at 20,0009xg for 30 min. The cleared supernatant was applied to amylose beads (NEB, Inc, USA), and protein was eluted with buffer 25 mM Tris–HCl pH 8.0, 200 mM NaCl, 3 mM β-ME and 10 mM maltose. Eluted *Nl*Gr7 protein fractions were checked by SDS-PAGE (12%), and the pure fractions were pooled. The eluted *Nl*Gr7 protein fractions were applied on a 10 kDa cut-off Centricon centrifugal device (Merck Pte. Ltd., Germany) for desalting against buffer (25 mM Tris–HCl, pH 8.0, 10 mM NaCl) and were concentrated to 56.75 mg/ml.

Cleavage of the MBP tag from *Nl*Gr7 was completed according to manual instructions of the pMAL protein fusion and purification system (NEB, Inc, USA). The tag (MBP) was removed by incubating with Factor Xa at 4°C for 3 h. The cleaved *Nl*Gr7 protein was concentrated by using a 10 kDa cut-off Centricon centrifugal device (Merck Pte. Ltd., Germany) and was purified by affinity chromatography on amylose resin (NEB, Inc, USA)

bioRxiv preprint doi: https://doi.org/10.1101/2020.09.05.284208; this version posted September 6, 2020. The copyright holder for this preprint (which was not certified by peer review) is the author/funder. All rights reserved. No reuse allowed without permission.

equilibrated with 20 mM Tris-HCl, pH 8.0, 200 mM NaCl, and 2 mM DTT; then, it was purified by a benzamidine column (GE Healthcare, USA) equilibrated with 20 mM Tris-HCl, pH 8.0, 200 mM NaCl and 2 mM DTT. Unbound *Nl*Gr7 fractions were checked by SDS-PAGE and were concentrated to 10.00 mg/ml and stored at -80°C. Subsequently, the purified protein of *Nl*Gr7 was analysed using LC-MS/MS (Q-TOF). The labelling of *Nl*Gr7 with biotin was completed as described by Ojha et al (2014). The expression and purification of the MBP (as a control protein) was completed as described above. The protein was concentrated to 61.77 mg/ml and stored at -80°C.

Protein-lectin-binding assay

To study lectin binding with *Nl*Gr7, 96-well Nunc microtiter plates (Fisher Scientific, Waltham, MA) were coated with *Nl*Gr7 in (100 ng; 50 µl/well) overnight (15-16 h, at 4°C). The plates were washed to remove unbound proteins, were blocked with 3% bovine albumin serum in Tris buffer and were incubated for 2 h at 100 rpm at room temperature. Additional biotinylated lectins (20 µg/ 50 µl; Vector Labs, Burlingame, CA) were added to each well and were incubated for 2 h at room temperature. Then, the plates were washed thrice with Tris buffer containing 0.05% Tween-20 to remove unbound or weakly bound biotinylated lectins, followed by incubation with streptavidin-HRP (1:2,000, 1 h, room temperature). The HRP activity was measured using a 50 µl TMB substrate solution (TransGen Biotech Co., LTD, China) containing 0.06% of 30% v/v hydrogen peroxide (H_2O_2) in each well. After 20 min, the reaction was stopped by adding 50 µl sulfuric acid (0.5 N) to each well. The absorbance was measured at 450 nm using an ELISA plate reader. The appropriate negative control was included, and the tests were run in quadruplicate.

Protein lipid overlay (PLO) assay

To test the binding ability of MBP-*Nl*Gr7 and MBP to various lipids, the well-established protein-lipid overlay (PLO) assay was performed using PIP and sphingo strips (Molecular Probes, USA) according to the manufacturer's instructions. These strips contained 100 pmol of various phospholipids and sphingolipids, which were spotted and immobilized on a nitrocellulose membrane. The purified MBP-*Nl*Gr7 was overlaid on PIP and sphingo strips. The purified MBP was used as an experimental control. Approximately 25 µg/ml protein was incubated with the strips in TBS-T (contained 3% BSA, Biotechnology Co. Ltd, Guangzhou, Xiang Bo) overnight at 4°C. The strips were then washed with TBS-T/BSA three times with gentle agitation for 10 min each wash, at room temperature. The MBP-*Nl*Gr7 and MBP interaction with spotted lipids were detected by subsequently blocking the strips in TBS-T buffer (10 mM Tris, pH 7.5, 70 mM NaCl, and 0.1% Tween) with 3% BSA and then

bioRxiv preprint doi: https://doi.org/10.1101/2020.09.05.284208; this version posted September 6, 2020. The copyright holder for this preprint (which was not certified by peer review) is the author/funder. All rights reserved. No reuse allowed without permission.

incubating the strips in 1:2000 dilution of monoclonal anti-MPB-HRP antibody (NEB, Inc, USA) in a blocking buffer for 1 h at room temperature. After thorough washing, a horse reddish peroxidase signal was detected by using 3,3'-diaminobenzidine tetrahydrochloride (DAB, Thermo Scientific) to yield an insoluble brown product. The intensity of the signals was analysed by using ImageJ.

An electrophoretic mobility shift assay (EMSA) for a metal-binding assay

The metal-binding properties of *Nl*Gr7 were confirmed by mixing purified *Nl*Gr7 (approximately 0.75 μg/5 μl) with equal volumes of the following solutions: 0.5 mM (final concentration) EDTA or 0.015, 0.05, 0.15, 0.5, or 1.0 mM metals ($CuSO_4$, and $CaCl_2$). Each mixture was incubated for 30 min at 25°C, was added to 10 μl Laemmli sample buffer, and then was subjected to 12% SDS-PAGE under reducing/non-heating conditions. As a negative control, we used the maltose-binding protein for metal-binding assay.

ATPase activity assay with purified *Nl*Gr7

The ATPase activity assay was performed in 96-well microtitre plates by using an ATPase/GTPase activity assay kit (Sigma-Aldrich, USA) according to the manufacturer's instructions. An aliquot of *Nl*Gr7-purified protein (6.25, 12.5, 25, 50, 100 μg/well) was mixed with a 5 μl assay buffer to make 10 μl of the ATPase activity assay sample. The phosphate standards and blank control for colorimetric detection were prepared according to the manufacturer's instructions of the ATPase/GTPase activity assay kit. An aliquot of 30 μl reaction mix (made with 20 μl assay buffer plus 10 μl 4 mM ATP solution) was added into each ATPase activity assay sample. After incubation at room temperature for 30 min, 200 μl reagent was added to each sample to terminate the enzyme reaction, and all samples were incubated for an additional 20 min. At this step, the transparent reaction mix suddenly changed to a fine green endpoint colour. The colour intensity was measured on a microtitre plate reader at 620 nm. All the assays were repeated five times. The ATPase activity of *Nl*Gr7 was determined by using the mean value of the samples according to the linear regression of standards.

Polysaccharide (insoluble)-binding study

To identify the specific carbohydrate-binding conserved aromatic amino acid residues in the *Nl*Gr7 sequence, *Nl*Gr7 was aligned with known carbohydrate-binding homologs (**Duan et al., 2016**) to create multiple sequence alignments by using ClustalW (http://www.genome.jp/tools-bin/clustalw). Furthermore, *Nl*Gr7 binding to various insoluble polysaccharides was determined as described by Duan et al (2016). The polysaccharides that

bioRxiv preprint doi: https://doi.org/10.1101/2020.09.05.284208; this version posted September 6, 2020. The copyright holder for this preprint (which was not certified by peer review) is the author/funder. All rights reserved. No reuse allowed without permission.

were tested were chitin, agarose, Sephadex G-100, raw cassava starch (tapioca starch), alpha-cellulose, and xylan from corn cobs.

Tastant-binding assay

To study the tastant-binding determination with *Nl*Gr7, the tastant-binding assay with *Nl*Gr7 was performed in 96-well microtitre plates. Microtitre plates were coated with purified *Nl*Gr7 protein (100 ng per well, 100 µl) and incubated overnight (15-16 h, at 4°C). The unbound protein was washed off (flicking and flapping manner) thrice with Tris buffer (25 mM Tris, pH 8.0, 10 mM NaCl). Then, the unbound sites were blocked with 3% bovine albumin serum in Tris buffer and were incubated for 2 h at 100 rpm at room temperature. An additional 100 µl tastants (50, 25, and 12.5 mM) were added into each well and were incubated for 2 h at room temperature. Then, free tastants were washed off thrice with Tris buffer containing 0.05% Tween-20. Subsequently, the wells were incubated with 100 µl biotinylated *Nl*Gr7 (100 ng), followed by incubation with streptavidin-HRP (1: 2000, 1 h, room temperature). Finally, the colour was developed. The bound enzyme activity was measured using 100 µl TMB substrate solution (TransGen Biotech Co., LTD, China) containing 0.06% of 30% v/v hydrogen peroxide (H_2O_2) in each well. Due to the enzyme activity, a gradual increase in brilliant blue colour intensity with the increasing concentration of tastants was observed. After 20 min, the reaction was stopped by adding 100 µl sulfuric acid (0.5 N) to each well. In this step, the brilliant blue colour suddenly changed to a fine yellow endpoint colour. The absorbance was measured at 450 nm using an ELISA plate reader.

Results

Characterization of *Nl*Gr7

The truncated cDNA of *NlGr7* consisted of 730 nucleotide bases coding for 243 amino acids with a predicted molecular mass of 28.70 kDa (**Fig. S1**). The cDNA clone was designated *Nl*Gr7 (**Kui et al., 2018**). The estimated pI of the predicted protein *Nl*Gr7 was found to be 9.19. There were eleven polar and nine non-polar amino acid residues. The instability index, as computed by the ExPASy ProtParam tool, was 36.27, which classified the protein as a stable protein (**Fig. S1**). Bioinformatics analysis using the TOPCONS tool predicted the absence of a secretory signal sequence and transmembrane helices in *Nl*Gr7 (**Fig. S2**). *Nl*Gr7 showed a 20.69-22.62% variation in sequence identity with the known Grs sequence of insect pests (**Table S1**). Phylogenetic analysis of *Nl*Gr7 revealed the degree of relationship with respect to genes from other insects (beetle, flies, mosquitos, moths, and butterflies) (**Fig. 1**). However, this study clearly classified *Nl*Gr7 and other insect taxa into two large clades. We

bioRxiv preprint doi: https://doi.org/10.1101/2020.09.05.284208; this version posted September 6, 2020. The copyright holder for this preprint (which was not certified by peer review) is the author/funder. All rights reserved. No reuse allowed without permission.

232 employed the polymerase chain reaction to amplify 730 bp *NlGr7* amplicons. We then
233 cloned, expressed, and purified the amplified amplicons (data not shown). The apparent
234 molecular weight of our protein of interest showed a mobility shift of ~55.428 kDa on SDS-
235 PAGE due to a high (9.19) isoelectric point (pI) and the presence of hydrophobic amino acids
236 in the *Nl*Gr7 sequence. Furthermore, this purified ~55.428 kDa protein was confirmed to be
237 *Nl*Gr7 (**Fig. 2A**), which is a sugar transporter of the BPH, based on mass-spectrometry
238 (LCMS/MS-Q-TOF) (**Fig. S3**).

239 **Lectin affinity for *Nl*Gr7**

240 To study the affinity of lectins, which are carbohydrate-binding proteins with *Nl*Gr7, a total
241 of fourteen lectins, griffonia (Bandeiraea) simplicifolia lectin (GSL), Pisum sativum
242 agglutinin (PSA), Lens culinaris agglutinin (LCA), Phaseolus vulgaris erythroagglutinin
243 (PHA-E), Phaseolus vulgaris leucoagglutinin (PHA-L), Sophora japonica agglutinin (SJA),
244 wheat germ agglutinin (WGA), concanavalin A (ConA), soybean agglutinin (SBA), wheat
245 germ agglutinin (WGA), Dolichos biflorus agglutinin (DBA), Ulex europaeus agglutinin 1
246 (UEA1), Ricinus communis agglutinin 1 (RCA1, Ricin), and peanut agglutinin (PNA), were
247 demonstrated to have affinity for *Nl*Gr7. DBA revealed the highest affinity, while UEA1
248 showed the lowest affinity for *Nl*Gr7 (**Fig. 2B**). The standard deviation (SD) of a set of
249 absorbance values ranged from ±0.001 to ± 0.08 (**Fig. 2B**). These lectins may combine with
250 *Nl*Gr7 and likely play numerous roles in biological recognition phenomena involving cells,
251 carbohydrates, and proteins.

252 **Lipid affinity for *Nl*Gr7**

253 We screened the arrays of 30 lipids by using the protein-lipid overlay (PLO) assay. This lipid
254 screen showed that recombinant *Nl*Gr7 binds to several anionic phospholipids, including
255 PtdIns(3)P, PtdIns(4)P, PtdIns(5)P, PtdIns(3,5)P2, PtdIns(4,5)P2, PtdIns(3,4,5)P3,
256 phosphatidic acid (PtdOH), phosphatidyl-serine (PtdSer) (**Fig. 2C**) and a single strong signal
257 of sphingolipid sulfatide (sulfogalactosylceramide; GalCerI3-sulfate) (**Fig. 2D**).

258 **Metals affinity to *Nl*Gr7**

259 The metal-binding capability of *Nl*Gr7 was verified by a gel mobility shift assay. The purified
260 *Nl*Gr7 mixed with different concentrations of $CuSO_4$ and $CaCl_2$ was resolved on SDS-PAGE.
261 Compared with the mobility of *Nl*Gr7 in the presence of 1.0 mM EDTA, the mobility of
262 *Nl*Gr7 was slowed by the addition of 0.015 to 1.0 mM $CuSO_4$. The migration of *Nl*Gr7
263 appeared to slow when the concentration of $CuSO_4$ was high (**Fig. 3A**), which suggested that
264 *Nl*Gr7 has the ability to bind Cu^{2+}. Furthermore, the copper-binding site, as predicted by the
265 RaptorX-binding server (http://raptorx.uchicago.edu/BindingSite), was interesting for the

bioRxiv preprint doi: https://doi.org/10.1101/2020.09.05.284208; this version posted September 6, 2020. The copyright holder for this preprint (which was not certified by peer review) is the author/funder. All rights reserved. No reuse allowed without permission.

observation of glutamine (Q)-64, asparagine (N)-117, lysine (K)-218, glutamine (Q)-222, threonine (T)-225, tyrosine (Y)-226, and isoleucine (I)-229 in the *Nl*Gr7 domain (**Fig. 3B**). The mobility of *Nl*Gr7 shifted with the addition of $CaCl_2$ in comparison with the mobility of *Nl*Gr7 in the presence of 1.0 mM EDTA (**Fig. S4**). On SDS-PAGE, the calcium-*Nl*Gr7 complex was stable in the presence of a low (0.015 and 0.05 mM) $CaCl_2$ concentration. At the same time, the calcium-*Nl*Gr7 complex was reduced in the presence of increasing (0.15, 0.5, and 1.0 mM) concentrations of $CaCl_2$ (**Fig. S4**). This reduced intensity of the calcium-*Nl*Gr7 complex on SDS-PAGE was due to the precipitation of the *Nl*Gr7 protein in the presence of a high concentration of calcium chloride under incubation for 30 min at 25°C.

Hydrolysis of the *Nl*Gr7-bound ATP

To understand how the predicted active site of *Nl*Gr7 might relate to its biological function, we investigated its biochemical activities *in vitro*. A total of 4 phosphorylated sites (serine (S)-54, tyrosine (Y)-104, tyrosine (Y)-105, and threonine (T)-201) and their corresponding catalytic protein kinases were predicted from the *Nl*Gr7 amino acid (1-243) sequence (http://kinasePhos.mbc.nctu.edu.tw/, **Fig. S5**). Furthermore, the developed phosphate standard curve showed that phosphate could be detected at a minimum of 500 pmol and maximum of 2000 pmol. The R^2 value was 0.992, as shown in the figure (**Fig. 3C, Table S2A**). Examination of the ATPase activity assay of bound phosphate in *Nl*Gr7 showed that 217.68-1125.85 pmol of phosphate was liberated (**Fig. 3D, Table S2B**), and its respective stable dark green colour with free phosphate liberated by the enzyme in a colorimetric product is shown in the figure (**Fig. 3E**). The R^2 value was 0.994, as shown in the figure (**Fig. 3D**). These data are consistent with the finding that *Nl*Gr7 displays its ATPase activity *in vitro*. We postulated that phosphate binding plays an important biochemical function.

***Nl*Gr7 exhibited polysaccharide (insoluble) specificity**

The purified *Nl*Gr7 showed a binding affinity for six insoluble polysaccharides. *Nl*Gr7 showed the highest affinity for tapioca starch, while *Nl*Gr7 showed the lowest affinity for Sephadex G-100 (**Fig. 4A**). Furthermore, seven carbohydrate-binding homologs sequences (**Duan et al., 2016**), belonging to accession numbers ADR64668-2, AFN57700-2, $CBM_{C5614-1}$, ADR64664, ADR64668-1, AFN57700-1, and CAJ19146, were aligned with *Nl*Gr7 to observe conserved aromatic amino acids, which were accepted to play an essential role in identifying and binding to polysaccharides. Two (Tryptophan (W)-59, and W-128) aromatic amino acids were identified as being completely conserved in all the aligned-sequences (numbered according to amino acids in *Nl*Gr7) (**Fig. 4B**, Red box). At the same time, phenylalanine (F)-91, tyrosine (Y)-104, F-108, and F-111 were observed to be partially

bioRxiv preprint doi: https://doi.org/10.1101/2020.09.05.284208; this version posted September 6, 2020. The copyright holder for this preprint (which was not certified by peer review) is the author/funder. All rights reserved. No reuse allowed without permission.

conserved aromatic amino acids in all the aligned sequences (**Fig. 4B**, Pink box). A phylogenetic tree revealed that *Nl*Gr7 showed the least similarity with other known carbohydrate-binding homolog sequences (**Fig. 4C**).

***Nl*Gr7 showed an interaction with various tastants**

Twelve tastants (D-(+) glucose, maltose, sucrose, D-(+) galactose, D-xylose, trehalose, D-(-) ribose, D-(-) melezitose, maltotriose, D-sorbitol, D-cellobiose, and myoinositol) were individually analysed, and all showed binding affinity for *Nl*Gr7 (**Fig. 5**). The binding affinities of the tastant preparations at each of the 3 concentrations of 50, 25, and 12.5 mM are depicted in Figure 5. Among the tastants, 50 mM D-cellobiose showed the highest (absorbance 0.352) binding affinity for *Nl*Gr7 (**Fig. 5K**), while 50 mM sorbitol showed the lowest (absorbance 0.065) binding affinity for *Nl*Gr7 (**Fig. 5J**). The standard deviation (SD) of a set of absorbance values ranged from ±0.0005 to ± 0.042 (**Fig. 5**).

Discussion

Here, we systematically characterized the functional properties of *NI*Gr7 using the macromolecular (*in vitro*) approach. Our study begins to overcome challenges in studying this highly divergent superfamily of insect Gr proteins and provides a systematic overview of ligand (metals, carbohydrates, lipids, lectins, and tastants) detection and ATP binding by this sugar receptor. The majority of gustatory receptor ligands in *Drosophila* have been studied by using electrophysiology recordings and/or behavioural investigations. However, there is, to some extent, a gap in the accurate interpretations of the electro-physiological data and behaviours that are recorded between wild-type and Gr mutant flies (**Miyamoto et al., 2013**).

The lectin-binding proteins of the rice brown planthopper are still undefined. Primary information from the BPH gustatory receptor and the lectin(s)-binding study reveals that the structure that interacts with the lectin(s) consists of carbohydrate moieties (**Lis and Sharon, 1986**). A variety of carbohydrate specificity-lectin(s) were selected for study (**Fig. 2B**). In assays, the *Nl*Gr7 protein interacted with a variety of sugar-specific lectins, which offers a complex oligosaccharide structure. Similar facts were found earlier for the human parotid salivary gland (**Rohringer and Holden, 1985**). The role that lectin-binding with *Nl*Gr7 (protein) plays in the developmental stages of the BPH has yet to be determined.

Although phospholipids (PLs) are only a minor nutrient compared to starch and protein, they may have both nutritional and functional significance. Phosphatidylcholine (PC), phosphatidylethanolamine (PE), phosphatidylinositol (PI) and their lyso forms are the major PLs in rice. Two PLs, PtdIns4P (phosphatidylinositol monophosphate) and PtdIns(4,5)P2

bioRxiv preprint doi: https://doi.org/10.1101/2020.09.05.284208; this version posted September 6, 2020. The copyright holder for this preprint (which was not certified by peer review) is the author/funder. All rights reserved. No reuse allowed without permission.

(phosphatidylinositol bisphosphate), have been reported as key intermediate sources of second messengers, and they directly affect the signal pathways in many animal cells and plants cells (**Chen et al., 1991**). In this study, *Nl*Gr7 binds to various lipids with different affinities and specificities (**Fig. 2C, D**), which could be the result of non-specific electrostatic interactions. The noticed affinities of *Nl*Gr7 for the lipids are specifically known as PH (pleckstrin homology) lipid-binding domains (**Stahelin, 2009**). However, various examples in prior studies show that low-affinity interactions have a distinct and influential impact on biological roles (**Becker et al., 1996**; **Irwin and Tan, 2014**; **Wilson, 2003**). Our rationale, which can be noticed in *Nl*Gr7-lipid interactions and in the lipids with their reported biological functions, reveals that lipid binding targets the chaperone proteins to specific cellular locations, where, in addition to participating in transmembrane targeting and protein folding, they also affect the physiological pathway of the membrane. Hence, the specific binding of lipids suggests that lipid binding has been a conserved function of *Nl*Gr7 since its appearance (**Fig. 2C, D**).

Copper is an important micronutrient that plays an essential role in plant growth and development (**Roy, 1931**); little is known about copper in insects. Insects often consume heavy metal ions from their niche. Previous reports revealed that copper is related to both the developmental stage of the organism, when animals undergo the transition from larval to adult blood types (**Durstewitz and Terwilliger, 1997**; **Ye et al., 2015**; **Li et al., 2016**), and the moulting cycle, when large fluctuations in protein synthesis take place (**Ye et al., 2015**; **Li et al., 2016**). In the present study, *Nl*Gr7 showed an interaction with copper. Therefore, taking this observation further, we speculate that copper may also play a role in the developmental stage (egg to adult) and moulting cycle of BPH. However, this has yet to be verified.

It has been noted that effectors from herbivores, which can bind to Ca^{2+}, are involved in suppressing the plant's defence (**Atamian et al., 2013**) and contracting forisomes (**Will et al., 2007**). However, the physiological mechanism of effector-mediated regulation of plant defences remains widely unexplained (**Consales et al., 2012**). The structure of the transduction pathway in gustation is unclear. The signalling pathways, including cGMP (**Amakawa et al., 1990**), inositol 1,4,5-triphosphate (IP_3) (**Koganezawa and Shimada, 2002**), and the sugar-receptor protein-gated channel (**Murakami and Kijima, 2000**), have been studied in few insects. Furthermore, GPCRs activate a temporal rise in intracellular Ca^{2+} because inositol 1,4,5-triphosphate activates delivery of Ca^{2+} from intracellular storage (**Torfs et al., 2002**). Therefore, we speculate that the GPCRs-IP_3-Ca^{2+}-mediated network may

bioRxiv preprint doi: https://doi.org/10.1101/2020.09.05.284208; this version posted September 6, 2020. The copyright holder for this preprint (which was not certified by peer review) is the author/funder. All rights reserved. No reuse allowed without permission.

impact the regulation of ligand-mediated calcium flux in the BPH physiological mechanism, but this has yet to be elucidated.

Polysaccharides display a wide range of solubility in water. However, some are water insoluble, e.g., chitin, agarose, tapioca starch, alpha cellulose, and xylan. Cellulose and chitin polysaccharides play structural roles in plants, fungi, and insects. The interactions between proteins and cellulose (**Georgelis et al., 2012**; **Boraston et al., 2004**; **Boraston, 2004**), as well as between human chitin-binding proteins (YKL-39 and -40) (**Schimpl et al., 2012**), have been studied extensively. However, the physiological role of these proteins remains poorly understood. Our results revealed a new carbohydrate-binding protein, *Nl*Gr7, which targets different insoluble polysaccharides that adopt varied conformations, including chitin, agarose, tapioca starch, alpha cellulose, and xylan. This study reveals that *Nl*Gr7 may possess higher plasticity to accommodate varied ligand conformations. This varied binding specificity remains unexplored without a structural study of the *Nl*Gr7-ligand complex, and it has yet to be a priority in future studies.

To study *Nl*Gr7 as a sugar Gr, we tested three different concentrations of twelve sugars to reveal the receptor's ligands. The results revealed that all 12 sugars interacted with *Nl*Gr7 (**Fig. 5**). A previous report demonstrated that galactose, xylose, glucose, and trehalose can regulate intracellular Ca^{2+} levels in insect cell lines (**Chen et al., 2019**; **Xu et al., 2012**). We speculate that expression of *Nl*Gr7 within the BPH may regulate the expression, localization, and/or function of the endogenous taste receptors of the BPH, thus leading to an increase or decrease in the responses to tastants.

Conclusions

Currently, there is insufficient knowledge about the function of gustatory (sugar) receptors within the insect. In a previous study in *Drosophila*, Gr43a showed upregulation during the feeding experiences of hungry flies and downregulation during feeding experiences in satiated flies (**Miyamoto et al., 2012**). In the present study, we observed the functional versatility of *Nl*Gr7. We assume that *Nl*Gr7 binding with its ligands may likely stimulate the physiological pathways of the BPH for feeding behaviour and adaptation. These observations extended our knowledge of the Grs (proteins) mechanism in insect and pest control.

Author contributions

WZ and AO conceived and designed the experiments. AO performed the experiments and analyzed the data. AO and WZ wrote the manuscript. Both authors have read and approved the final manuscript.

bioRxiv preprint doi: https://doi.org/10.1101/2020.09.05.284208; this version posted September 6, 2020. The copyright holder for this preprint (which was not certified by peer review) is the author/funder. All rights reserved. No reuse allowed without permission.

Acknowledgements

We thank Longgyu Yuan for their assistance with insect maintaining in green house at State Key Laboratory of Biocontrol, SunYat-sen University, China.

Competing interests

The authors declared that they have no competing or financial interest.

Funding

This work was funded by the National Natural Science Foundation of China (U1401212) to WZ. AO thanks the State Key Laboratory of Biocontrol visiting scholar foundation for a research grant (SKLBC15F02), SunYat-sen University, China.

References

1. Amakawa, T., Ozaki, M. and Kawata, K. (1990). Effects of cyclic GMP on the sugar taste recepStor cell of the fly *Phormia regina*. J. Insect Physiol. **36**, 281–286.

2. Amrein, H. and Thorne, N. (2005). Gustatory perception and behavior in *Drosophila melanogaster*. Curr. Biol. **15**(17), R673-684.

3. Atamian, H. S., Chaudhary, R., Cin, V. D., Bao, E., Girke, T. and Kaloshian, I. (2013). In planta expression or delivery of potato aphid *Macrosiphum euphorbiae* effectors Me10 and Me23 enhances aphid fecundity. Mol. Plant Microbe Interact. **26**(1), 67-74.

4. Becker, T. C., Noel, R. J., Johnson, J. H., Lynch, R. M., Hirose, H., Tokuyama, Y., Bell, G. I. and Newgard, C. B. (1996). Differential effects of overexpressed glucokinase and hexokinase I in isolated islets. Evidence for functional segregation of the high and low Km enzymes. J. Biol. Chem. **271**(1), 390-394.

5. Benton, R., Sachse, S., Michnick, S. W. and Vosshall, L. B. (2006). Atypical membrane topology and heteromeric function of *Drosophila* odorant receptors in vivo. PLoS Biol. **4**(2), e20.

6. Boraston, A. B. (2005). The interaction of carbohydrate-binding modules with insoluble non-crystalline cellulose is enthalpically driven. Biochem. J. **385**(Pt2), 479-484.

7. Boraston, A. B., Bolam, D. N., Gilbert, H. J. and Davies, G. J. (2004). Carbohydrate-binding modules: fine-tuning polysaccharide recognition. Biochem. J. **382**(Pt3), 769-781.

bioRxiv preprint doi: https://doi.org/10.1101/2020.09.05.284208; this version posted September 6, 2020. The copyright holder for this preprint (which was not certified by peer review) is the author/funder. All rights reserved. No reuse allowed without permission.

8. Chen, Q., Brglez, I. and Boss, W. F. (1991). Inositol phospholipids as plant second messengers. Symp. Soc. Exp. Biol. **45**, 159-175.

9. Chen, W. W., Kang, K., Yang, P. and Zhang, W. Q. (2019). Identification of a sugar gustatory receptor and its effect on fecundity of the brown planthopper *Nilaparvata lugens*. Insect Sci. **26**(3), 441-452.

10. Clyne, P. J., Warr, C. G. and Carlson, J. R. (2000). Candidate taste receptors in *Drosophila*. Science **287**(5459), 1830-1834.

11. Consales, F., Schweizer, F., Erb, M., Gouhier-Darimont, C., Bodenhausen, N., Bruessow, F., Sobhy, I. and Reymond, P. (2012). Insect oral secretions suppress wound-induced responses in *Arabidopsis*. J. Exp. Bot. **63**(2), 727-737.

12. Dahanukar, A., Foster, K., van der Goes van Naters, W. M. and Carlson, J. R. (2001). A Gr receptor is required for response to the sugar trehalose in taste neurons of *Drosophila*. Nat. Neurosci. **4**(12), 1182-1186.

13. Dahanukar, A., Lei, Y. T., Kwon, J. Y. and Carlson, J. R. (2007). Two Gr genes underlie sugar reception in *Drosophila*. Neuron **56**(3), 503-516.

14. Duan, C. J., Feng, Y. L., Cao, Q. L., Huang, M. Y. and Feng, J. X. (2016). Identification of a novel family of carbohydrate-binding modules with broad ligand specificity. Sci. Rep. **6**, 19392.

15. Dunipace, L., Meister, S., McNealy, C. and Amrein, H. (2001). Spatially restricted expression of candidate taste receptors in the *Drosophila* gustatory system. Curr. Biol. **11**(11), 822-835.

16. Durstewitz, G. and Terwilliger, N. B. (1997). Developmental changes in hemocyanin expression in the Dungeness crab, *Cancer magister*. J. Biol. Chem. **272**(7), 4347-4350.

17. Gardiner, A., Barker, D., Butlin, R. K., Jordan, W. C. and Ritchie, M. G. (2008). Evolution of a complex locus: exon gain, loss and divergence at the Gr39a locus in *Drosophila*. PLoS One **3**(1), e1513.

18. Georgelis, N., Yennawar, N. H. and Cosgrove, D. J. (2012). Structural basis for entropy-driven cellulose binding by a type-A cellulose-binding module (CBM) and bacterial expansin. Proc. Natl. Acad. Sci. U.S.A. **109**(37), 14830-14835.

bioRxiv preprint doi: https://doi.org/10.1101/2020.09.05.284208; this version posted September 6, 2020. The copyright holder for this preprint (which was not certified by peer review) is the author/funder. All rights reserved. No reuse allowed without permission.

460 19. Hill, C. A., Fox, A. N., Pitts, R. J., Kent, L. B., Tan, P. L., Chrystal, M. A., Cravchik, A.,
461 Collin, F. H., Robertson, H. M. and Zwiebel, L. J. (2002). G protein coupled receptors
462 in *Anopheles gambiae*. Science **298**(5591), 176-178.

463 20. Irwin, D. M. and Tan, H. (2014). Evolution of glucose utilization: glucokinase and
464 glucokinase regulator protein. Mol. Phylogenet. Evol. **70,** 195-203.

465 21. Kent, L. B., Walden, K. K. and Robertson, H. M. (2008). The gr family of candidate
466 gustatory and olfactory receptors in the yellow-fever mosquito *Aedes aegypti*. Chem.
467 Senses **33**(1), 79-93.

468 22. Koganezawa, M. and Shimada, l. (2002). Inositol 1,4,5-trisphosphate transduction
469 cascade in taste reception of the fleshfly, *Boettcherisca peregrina*. J. Neurobiol. **51**, 66-
470 83.

471 23. Kang, K., Yang, P., Chen, L. E., Pang, R., Yu, L. J., Zhou, W. W., Zhu, Z. R. and Zhang,
472 W. Q. (2018). Identification of putative fecundity-related gustatory receptor genes in the
473 brown planthopper *Nilaparvata lugens*. BMC Genomics **19**(1): 970.

474 24. Lee, Y., Moon, S. J. and Montell, C. (2009). Multiple gustatory receptors required for the
475 caffeine response in *Drosophila*. Proc. Natl. Acad. Sci. U.S.A. **106**(11), 4495-4500.

476 25. Li, Z., An, X. K., Liu, Y. D. and Hou, M. L. (2016). Transcriptomic and expression
477 analysis of the salivary glands in white-backed planthoppers, *Sogatella furcifera*. PLoS
478 One **11**(7), e0159393.

479 26. Lis, H. and Sharon, N. (1986). Lectins as molecules and as tools. Annu. Rev. Biochem.
480 **55,** 35-67.

481 27. Miyamoto, T., Chen, Y. and Slone, J. (2013). Identification of a *Drosophila* glucose
482 receptor using Ca2+ imaging of single chemosensory neurons. PLoS ONE **8**(2), e56304.

483 28. Miyamoto, T., Slone, J., Song, X. and Amrein, H. (2012). A fructose receptor functions
484 as a nutrient sensor in the *Drosophila* brain. Cell **151**(5), 1113-1125.

485 29. Murakami, M. and Kijima, H. (2000). Transduction ion channels directly gated by sugars
486 on the insect taste cell. J. Gen. Physiol. **115**, 455-466.

bioRxiv preprint doi: https://doi.org/10.1101/2020.09.05.284208; this version posted September 6, 2020. The copyright holder for this preprint (which was not certified by peer review) is the author/funder. All rights reserved. No reuse allowed without permission.

30. Ojha, A., Sree, K. S., Sachdev, B., Rashmi, M. A., Ravi, K. C., Suresh, P. J., Mohan, K. S. and Bhatnagar, R. K. (2014). Analysis of resistance to Cry1Ac in field-collected pink bollworm, *Pectinophora gossypiela* (Lepidoptera: Gelechiidae), populations. GM Crops Food **5**(4), 280-286.

31. Ojha, A. and Zhang, W. Q. (2019). A comparative study of microbial community and dynamics of *Asaia* in the brown planthopper from susceptible and resistant rice varieties. BMC Microbiol. **19**(1), 139.

32. Robertson, H. M., Warr, C. G. and Carlson, J. R. (2003). Molecular evolution of the insect chemoreceptor gene superfamily in *Drosophila melanogaster*. Proc. Natl. Acad. Sci. U.S.A. **100**(Suppl 2), 14537-14542.

33. Robertson, H. M. and Wanner, K. W. (2006). The chemoreceptor superfamily in the honey bee, *Apis mellifera*: expansion of the odorant, but not gustatory, receptor family. Genome Res. **16**(11), 1395-1403.

34. Rohringer, R and Holden, D. W. (1985). Protein blotting: detection of proteins with colloidal gold, and of glycoproteins and lectins with biotin-conjugated and enzyme probes. Anal. Biochem. **144**(1), 118-127.

35. Roy, M. (1931). A quantitative study of copper in insects. Annals of the Entomological Society of America **24**(3), 485-488.

36. Schimpl, M., Rush, C. L., Betou, M., Eggleston, I. M., Recklies A. D. and van Aalten, D. M. (2012). Human YKL-39 is a pseudo-chitinase with retained chitooligosaccharide-binding properties. Biochem. J. **446**(1), 149-57.

37. Shankar, S., Chua, J. Y., Tan, K. J., Calvert, M. E., Weng, R., Ng, W. C., Mori, K. and Yew, J. Y. (2015). The neuropeptide tachykinin is essential for pheromone detection in a gustatory neural circuit. Elife **4**, e06914.

38. Slone, J., Daniels, J. and Amrein, H. (2007). Sugar receptors in *Drosophila*. Curr. Biol. **17**(20), 1809-1816.

39. Smadja, C., Shi, P., Butlin, R. K. and Robertson, H. M. (2009). Large gene family expansions and adaptive evolution for odorant and gustatory receptors in the pea aphid, *Acyrthosiphon pisum*. Mol. Biol. Evol. **26**(9), 2073-2086.

bioRxiv preprint doi: https://doi.org/10.1101/2020.09.05.284208; this version posted September 6, 2020. The copyright holder for this preprint (which was not certified by peer review) is the author/funder. All rights reserved. No reuse allowed without permission.

40. Stahelin, R. V. (2009). Lipid binding domains: more than simple lipid effectors. J. Lipid Res. **50**(Suppl), S299-S304.

41. Torfs, H., Poels, J., Detheux, M., Dupriez, V., Van Loy, T., Vercammen, L., Vassart, G., Parmentier, M. and Vanden Broeck, J. (2002). Recombinant aequorin as a reporter for receptor-mediated changes of intracellular Ca2+-levels in *Drosophila* S2 cells. Invert. Neurosci. **4**,119-124.

42. Tribolium Genome Sequencing Consortium, Richards, S., Gibbs, R. A., Weinstock, G. M., Brown, S. J., Denell, R., Beeman, R. W., Gibbs, R., Beeman, R. W., Brown, S. J. et al. (2008). The genome of the model beetle and pest *Tribolium castaneum*. Nature **452**(7190), 949-955.

43. Wanner, K. W. and Robertson, H. M. (2008). The gustatory receptor family in the silkworm moth *Bombyx mori* is characterized by a large expansion of a single lineage of putative bitter receptors. Insect Mol. Biol. **17**(6), 621-629.

44. Weiss, L. A., Dahanukar, A., Kwon, J. Y., Banerjee, D. and Carlson, J. R. (2011). The molecular and cellular basis of bitter taste in *Drosophila*. Neuron **69**(2), 258-272.

45. Will, T., Tjallingii, W. F., Thönnessen, A. and van Bel, A. J. (2007). Molecular sabotage of plant defense by aphid saliva. Proc. Natl. Acad. Sci. U.S.A. **104**(25), 10536-10541.

46. Wilson, J. E. (2003). Isozymes of mammalian hexokinase: structure, subcellular localization and metabolic function. J. Exp. Biol. **206**(Pt12), 2049-2057.

47. Xu, W., Papanicolaou, A., Zhang, H. J. and Anderson, A. (2016). Expansion of a bitter taste receptor family in a polyphagous insect herbivore. Sci. Rep. **6**, 23666.

48. Xu, W. and Anderson, A. (2015). Carbon dioxide receptor genes in cotton bollworm *Helicoverpa armigera*. Naturwissenschaften **102**(3-4), 11.

49. Xu, W., Zhang, H. J. and Anderson, A. (2012). A sugar gustatory receptor identified from the foregut of cotton bollworm *Helicoverpa armigera*. J. Chem. Ecol. **38**(12), 1513-1520.

50. Xue, J., Zhou, X., Zhang, C. X., Yu, L. L., Fan, H. W., Wang, Z., Xu, H. J., Xi, Y., Zhu, Z. R. and Zhou, Z. R. (2014). Genomes of the rice pest brown planthopper and its

bioRxiv preprint doi: https://doi.org/10.1101/2020.09.05.284208; this version posted September 6, 2020. The copyright holder for this preprint (which was not certified by peer review) is the author/funder. All rights reserved. No reuse allowed without permission.

545 endosymbionts reveal complex complementary contributions for host adaptation.
546 Genome Biol. **15**(12), 521.

547 51. Ye, Y. X., Pan, P. L., Kang, D., Lu, J. B. and Zhang, C. X. (2015). The multicopper
548 oxidase gene family in the brown planthopper, *Nilaparvata lugens*. Insect Biochem. Mol.
549 Biol. **63,** 124-132.

550 52. Zhang, H. J., Anderson, A. R., Trowell, S. C., Luo, A. R., Xiang, Z. H. and Xia, Q. Y.
551 (2011). Topological and functional characterization of an insect gustatory receptor. PLoS
552 One **6**(8), e24111.

553 **Figure legends**

554 **Figure 1**| Phylogenetic tree showing the relation between orthologues of gustatory receptor
555 reported from different organisms.

556 **Figure 2**| *Nl*Gr7 recombinant protein and *Nl*Gr7-ligands overlay assays. (A) Purified *Nl*Gr7,
557 (B) *Nl*Gr7-lectin overlay assay shows that *Nl*Gr7 binds to several lectins. Protein-lipid
558 overlay assay shows that *Nl*Gr7 binds to several anionic lipids. (C) *Nl*Gr7 reveals interaction
559 to phospholipids, and (D) interaction to sphingolipids.

560 **Figure 3**| Overview of the *Nl*Gr7-copper complex and ATPase/GTPase activity assay for
561 *Nl*Gr7. (A) The gel mobility shifts of the *Nl*Gr7-copper complex showed a varied range of
562 copper. (B) Predicted binding amino acid residues Q64, N117, K218, Q222, T225, Y226, and
563 I229 anchor copper within the *Nl*Gr7. (C) Standard curve prepared according to the
564 ATPase/GTPase activity kit instructions. (D) The *Nl*Gr7 (6.25, 12.5, 25, 50, or 100 μg)
565 determined ATP. (E) This ATPase/GTPase activity assay is a colorimetric test that shows the
566 amount of free inorganic phosphate (Pi). Controls that included no *Nl*Gr7 were measured to
567 observe for spontaneous ATP hydrolysis of ATP, and their optical density (OD) values were
568 deducted from the samples' values.

569 **Figure 4**| Characterization of *Nl*Gr7 as a novel carbohydrate protein. (A) Binding of *Nl*Gr7 to
570 insoluble polysaccharides. Thirty micrograms of purified *Nl*Gr7 was incubated with 200 μl
571 4% (wt/vol) insoluble polysaccharide including chitin, agarose, Sephadex G-100, raw cassava
572 starch (tapioca starch), alpha-cellulose, or xylan from corn cobs. The same amount of protein
573 used in the binding assay but without polysaccharide was included as a control (CK). (B)
574 Multiple sequence alignment of *Nl*Gr7 and selected carbohydrate-binding homologs. The

bioRxiv preprint doi: https://doi.org/10.1101/2020.09.05.284208; this version posted September 6, 2020. The copyright holder for this preprint (which was not certified by peer review) is the author/funder. All rights reserved. No reuse allowed without permission.

sequence similarity and identity are shown by dots and asterisks, respectively. Entirely conserved aromatic (tryptophan (W)-59, and W-128) amino acids are red, and partly conserved aromatic (phenylalanine (F)-91, tyrosine (Y)-104, F-108, and F-111) amino acids are pink. (C) Phylogenetic tree showing the relation between orthologues of the carbohydrate protein that was reported previously.

Figure 5| Tastants screening assay. The binding of *Nl*Gr7 to different concentrations (50, 25, and 12.5 mM) of tastants. (A) D-(+) glucose, (B) maltose, (C) sucrose, (D) D(+) galactose, (E) D-xylose, (F) trehalose, (G) D-(-) ribose, (H) D-(-) melezitose, (I) maltotriose, (J) D-sorbitol, (K) D-cellobiose, and (L) myoinositol.

Supplementary materials

Figure S1. The computation of various physical and chemical parameters of *Nl*Gr7.

Figure S2. Consensus prediction of membrane protein topology using the TOPCONS server indicated no trans-membrane helices (blue in the graph) in the predicted amino acid sequence of *Nl*Gr7. TOPCONS predicted the topology of *Nl*Gr7 from five different topology prediction algorithms: OCTOPUS, Philius, PolyPhobius, SCAMPI (multiple sequence mode), and SPOCTOPUS. The output of these five algorithms was used as input for the TOPCONS Hidden Markov Model (HMM) (shown in maroon), which provided a consensus prediction for the protein together with a reliability score based on the agreement of the included methods across the sequence. In addition, ZPRED was used to predict the Z-coordinate (i.e., the distance to the membrane centre) of each amino acid, and the G-scale was used to predict the free energy of the membrane insertion for a window of 19 amino acids that were centred around each position in the sequence.

Figure S3. LCMS/MS-Q-TOF-based identification of the *Nl*Gr7. (A) Parameters used in MASCOT search, (B and C) The green area is a significant threshold. This area of the score over the results of the identification of the mascot positive result**s**, (D and E) decoy search summary, and (F) cross-examination of the LCMS/MS-QTOF-generated peptide sequence of the sugar transporter sequence blast in the NCBI protein database.

Figure S4. An electrophoretic mobility shift assay (EMSA) for the calcium-binding assay.

Figure S5. Computationally predicted catalytic kinase-specific phosphorylation sites within the *Nl*Gr7 sequence using the KinasePhos tool.

bioRxiv preprint doi: https://doi.org/10.1101/2020.09.05.284208; this version posted September 6, 2020. The copyright holder for this preprint (which was not certified by peer review) is the author/funder. All rights reserved. No reuse allowed without permission.

Table S1. *Nl*Gr7 protein sequence identity with known chemoreceptors of insects.

Table S2. ATPase activity assay with *Nl*Gr7. Hydrolysis of the *Nl*Gr7-bound ATP. (A) Standard curve of phosphate, (B) the concentration of released phosphate from the *Nl*Gr7-bound ATP. The released concentration of phosphate from the samples per well was calculated using the phosphate standard curve value 500 pmol.

Figure 1

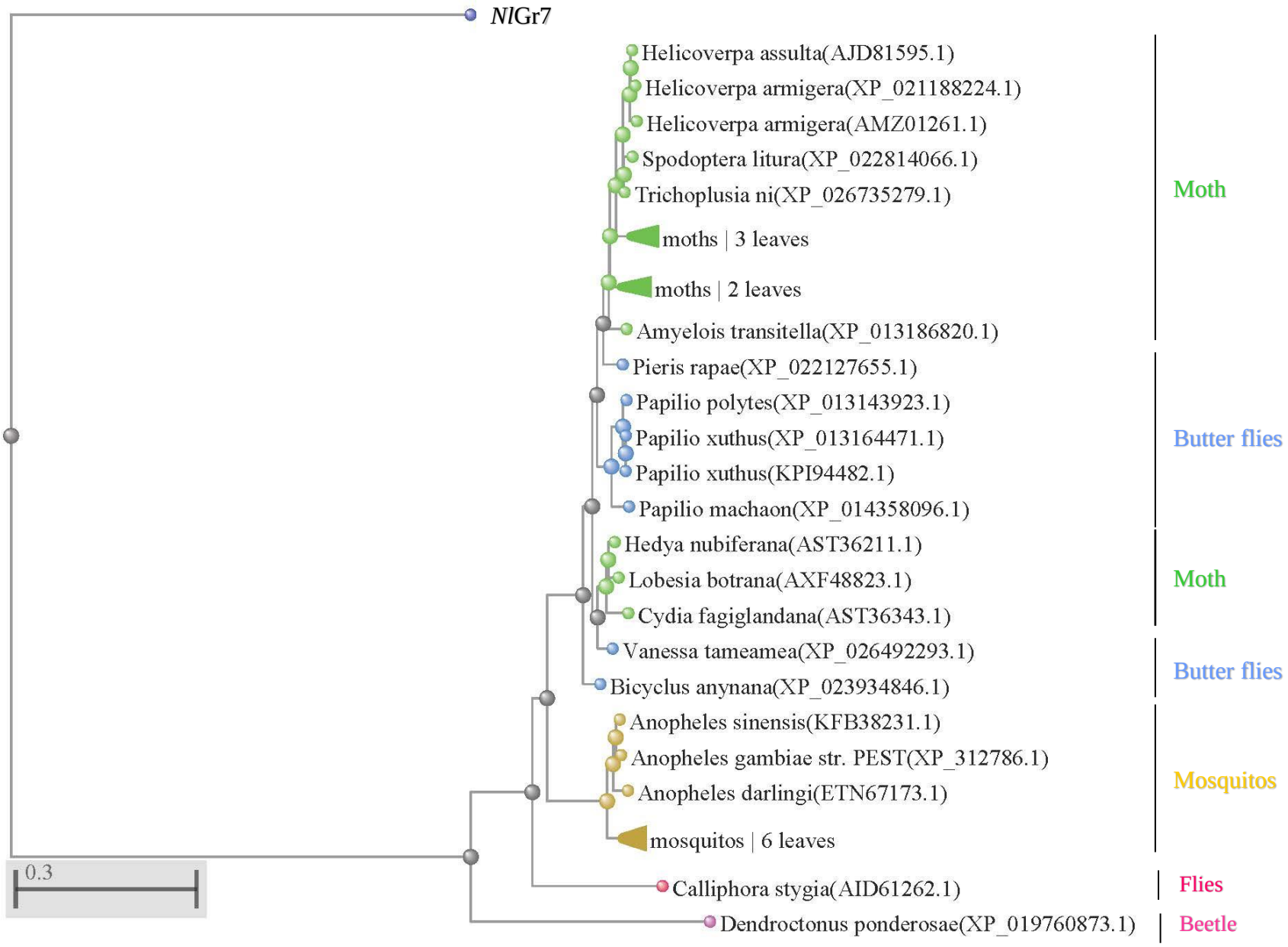
NlGr7
Helicoverpa assulta(AJD81595.1)
Helicoverpa armigera(XP_021188224.1)
Helicoverpa armigera(AMZ01261.1)
Spodoptera litura(XP_022814066.1)
Trichoplusia ni(XP_026735279.1)
moths | 3 leaves
moths | 2 leaves
Amyelois transitella(XP_013186820.1)
Pieris rapae(XP_022127655.1)
Papilio polytes(XP_013143923.1)
Papilio xuthus(XP_013164471.1)
Papilio xuthus(KPI94482.1)
Papilio machaon(XP_014358096.1)
Hedya nubiferana(AST36211.1)
Lobesia botrana(AXF48823.1)
Cydia fagiglandana(AST36343.1)
Vanessa tameamea(XP_026492293.1)
Bicyclus anynana(XP_023934846.1)
Anopheles sinensis(KFB38231.1)
Anopheles gambiae str. PEST(XP_312786.1)
Anopheles darlingi(ETN67173.1)
mosquitos | 6 leaves
Calliphora stygia(AID61262.1)
Dendroctonus ponderosae(XP_019760873.1)
0.3
Moth
Butter flies
Moth
Butter flies
Mosquitos
Flies
Beetle

Figure 2

A

B

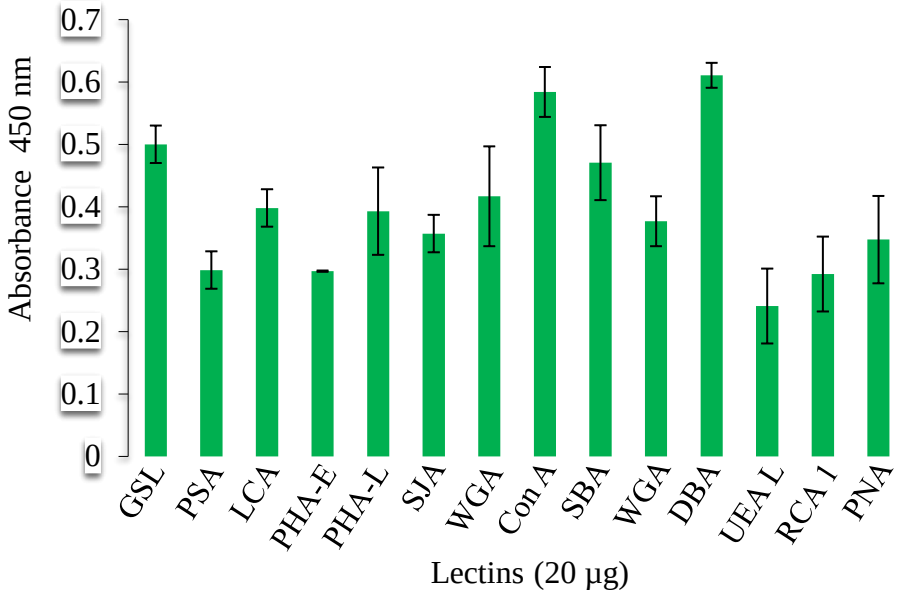

C

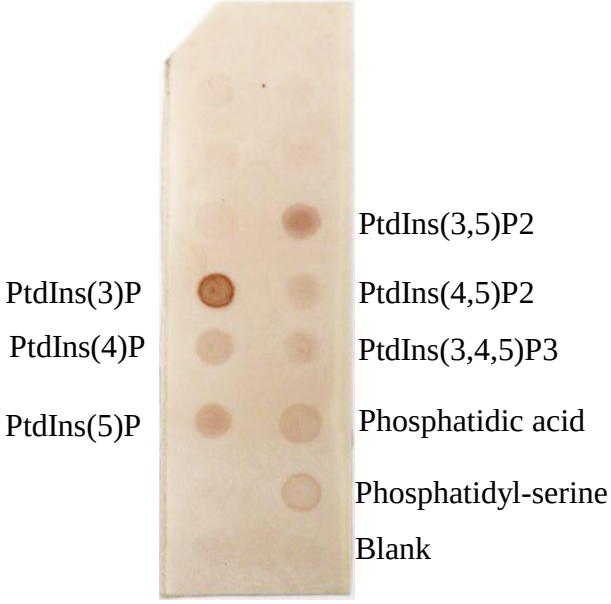

D

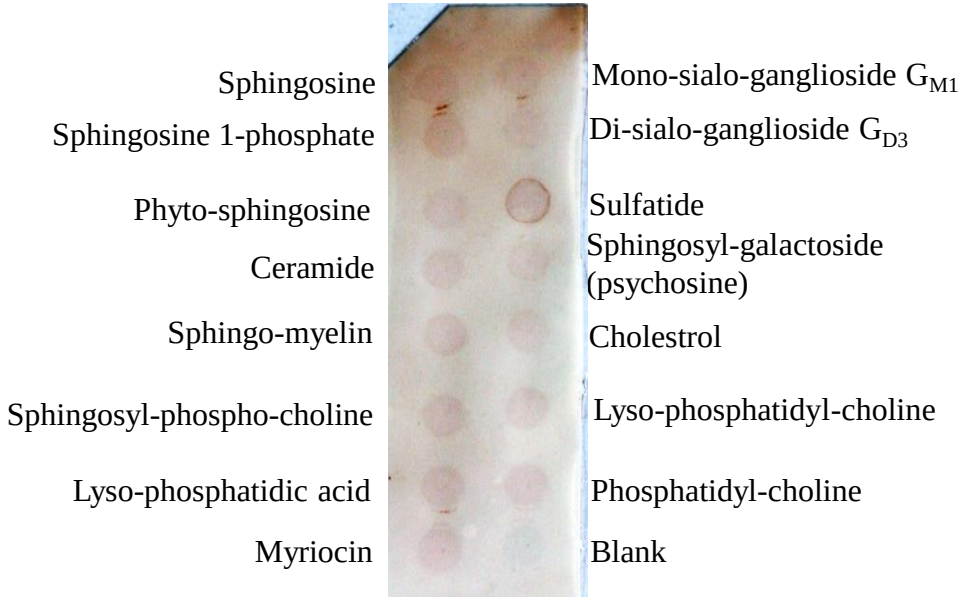

Figure 3

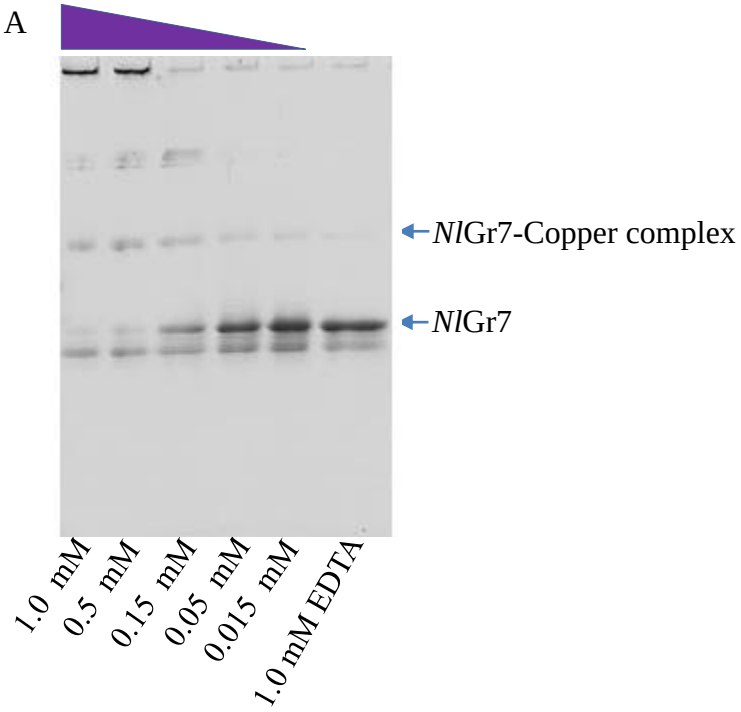
A
NlGr7-Copper complex
NlGr7
1.0 mM
0.5 mM
0.15 mM
0.05 mM
0.015 mM
1.0 mM EDTA

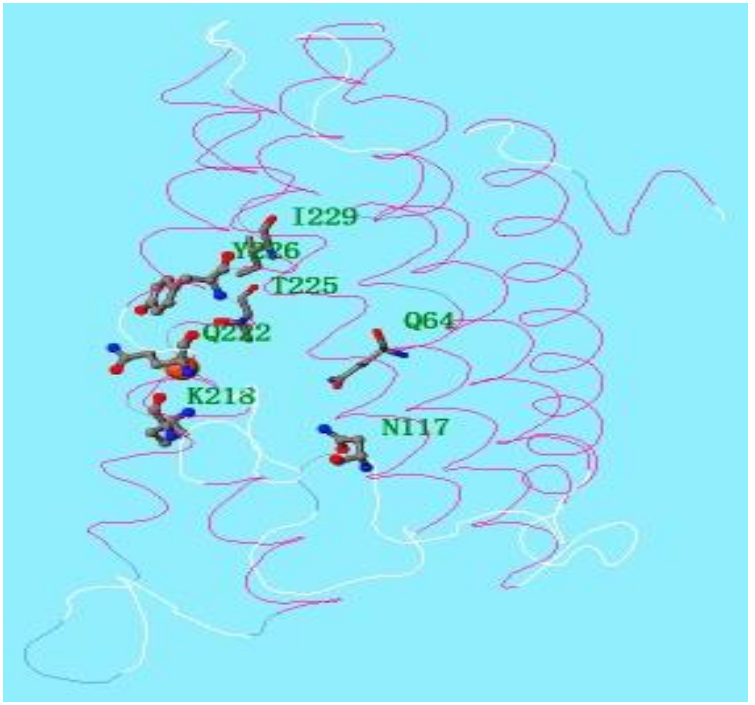
B
I229
T225
Q64
K218
N117

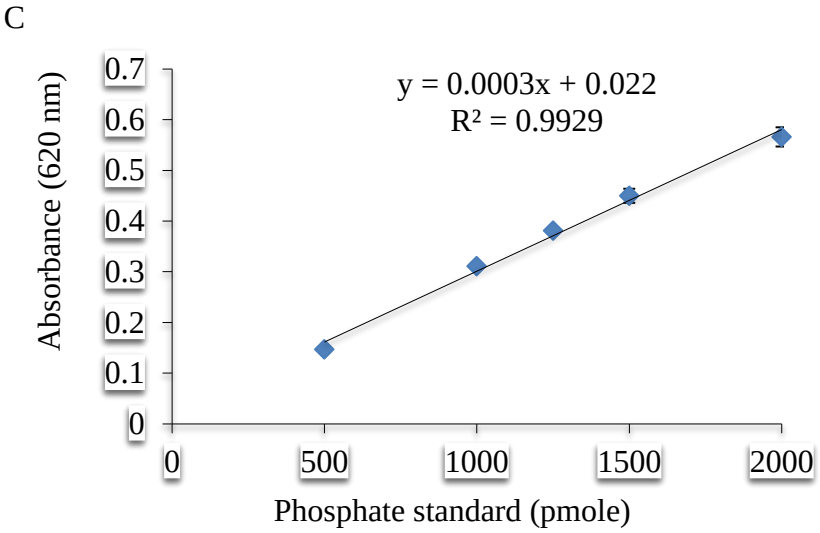
C
y = 0.0003x + 0.022
R² = 0.9929
Absorbance (620 nm)
Phosphate standard (pmole)

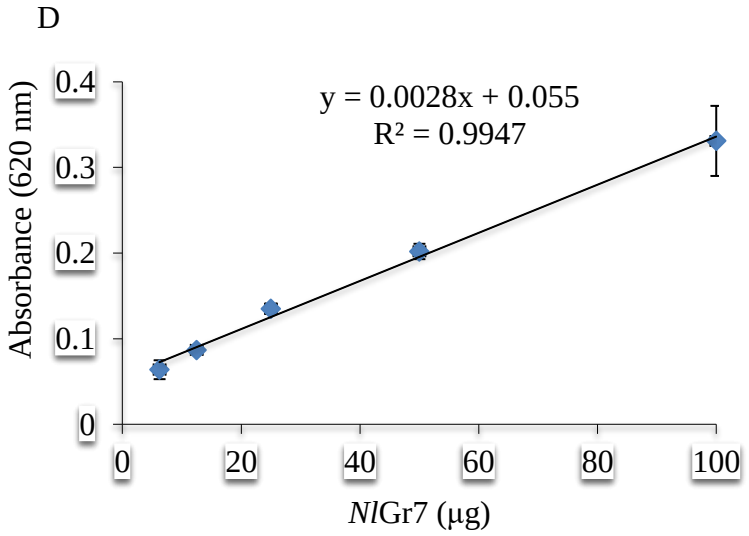
D
y = 0.0028x + 0.055
R² = 0.9947
Absorbance (620 nm)
NlGr7 (µg)


E
Blank
Blank

Figure 4

A

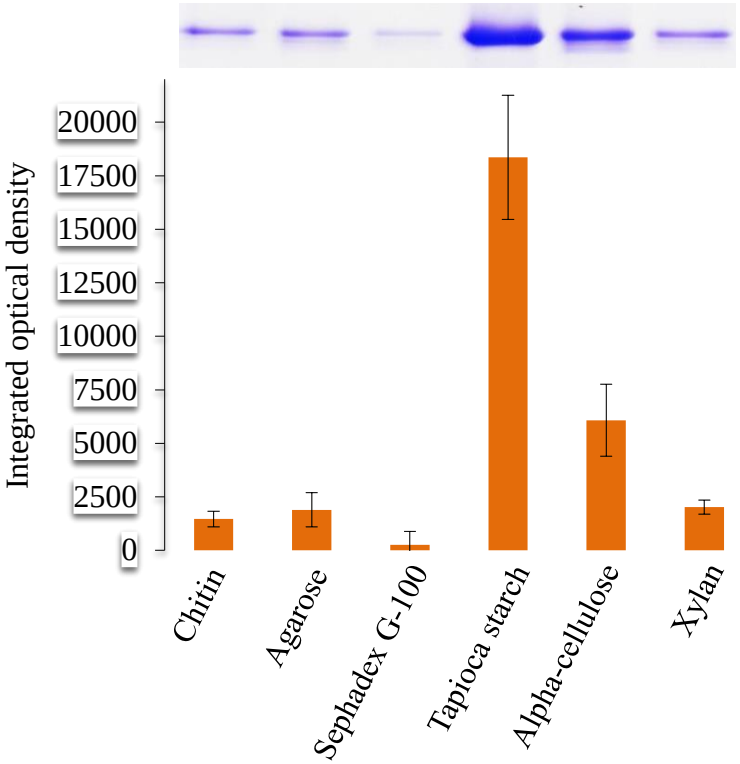

*Nl*Gr7 binding to insoluble polysaccharides

B

```
ADR64668-2  ----------------------------------------ETSEETVIFEGEQQLEWG  428
AFN57700-2  ----------------------------------------EAAKETVVFEGEQQLEWG  401
CBM C5614-1 ----------------------------------------DSSKGTVAFEGEKTLEWG  381
ADR64664    ----------------------------------------DSSKGTVVFEGEKTLDWG  350
ADR64668-1  ----------------------------------------GSGGETVFWEGDAVLDWG  566
AFN57700-1  ----------------------------------------EPAASEVFWEGDEMLDWG  537
CAJ19146    ----------------------------------------QALQPSVVYQGDELMNWG  422
NlGr7       LLLTIVLIFKHFLMIAVDMVCYLALKAVQNTSDQLIRHYKQIDMTKVSSERLNSYETIWF  60
                                                                  ..  *

ADR64668-2  Q--AVNFP------------------ANLFTNLSNTSTVEVTYTEKFDQFSGDEANSYL  467
AFN57700-2  G--AIQFP------------------SSLFDGLS-DAELELTYTEKFDQFEGGEANSYL  439
CBM C5614-1 E--GVFVP------------------SSMLTDVGEDVEVELTYKLDFTDYDD------I  414
ADR64664    Q--AVTVQ------------------ATSLADIGNKVEVELTYKLDYTDYDD------M  383
ADR64668-1  DGLQLTVP------------------AESFEAVGKGARLILSYTLDFTDYNM------I  601
AFN57700-1  DGLQLPIP------------------GERFENYGKDVKLIFHYTLDFTDYNM------I  572
CAJ19146    EGKQLIIA------------------GSKFAYFTAESKLMVTLDAEPGADYD-----ML  458
NlGr7       KLTQLLKNTVDYFPPLYTAVCLEGAIFTFSFVHLSIYHYSYSEYYMDFLQFREKGGN-IT  119
                :                        :                .

ADR64668-2  QFWYN--DWSSMVNFTADGGQEISETLEVVNKFYNSTSGTEHTTVFAFDKETFQNFKKKG  523
AFN57700-2  QFWYN--DWSSMINFTVDG-QEXNETLEVN-KFYNSTSGTDHTTLFTFDAETFKNFKKG-  495
CBM C5614-1 QFMYNNGGWQKIPSGLSMDGKAFDGADFSASSVYGIQSGDTKTSVLTFDASAYGYVSKYE  474
ADR64664    QFLYNKGGWQK------------------------------------------------  394
ADR64668-1  QLFYG--DWKDNPSFIINGKEIAKEFRPSD--LHGLKNGDDGVTEITFSDAVFDIILQKG  657
AFN57700-1  QLFYG--DWSSNPSFIINGQQIDKEFRPSD--VHGLKNGDDGVSELTFSEDVYNVIIAKG  628
CAJ19146    QFAYG--DWKSKPLMIISGRSYKGQVEPSK----INGSRNTYTLFIGFKESSLNQLKDKG  522
NlGr7       ESDHYIFDWYNVKQLHSTLLILLAVYYFRLWMIFRVCHGAQKQISGETKRQLQNIIADRI  179
            :  :   .* .

ADR64668-2  MLFQG---HGVLLKKVVLKAGEKDPD--------------------------------  546
AFN57700-2  MLFQG---HGVLLKKAVLKAKAKEGE--------------------------------  518
CBM C5614-1 MVIQG---HGVIMKKVTVRAPSGTSA--------------------------------  497
ADR64664    ----------------------------------------------------------  394
ADR64668-1  IVFQG---HGLRLKKVVLAGPATAIQ--------------------------------  680
AFN57700-1  IAVQG---HGLRLKKVELAGPESTGI--------------------------------  651
CAJ19146    ITLQG---HGLRLRNVVVMPEGLVLGL--------------------------------  536
NlGr7       IDNPGSETHAKHFLKRVSMRPTEILLHGRTTVNNYSFLKIALQILTYTIIIVHFKKMLTN  239
```

C

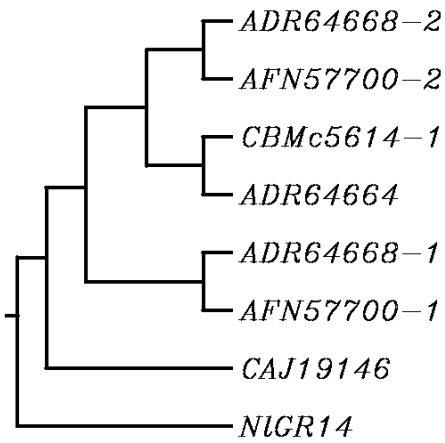

Figure 5

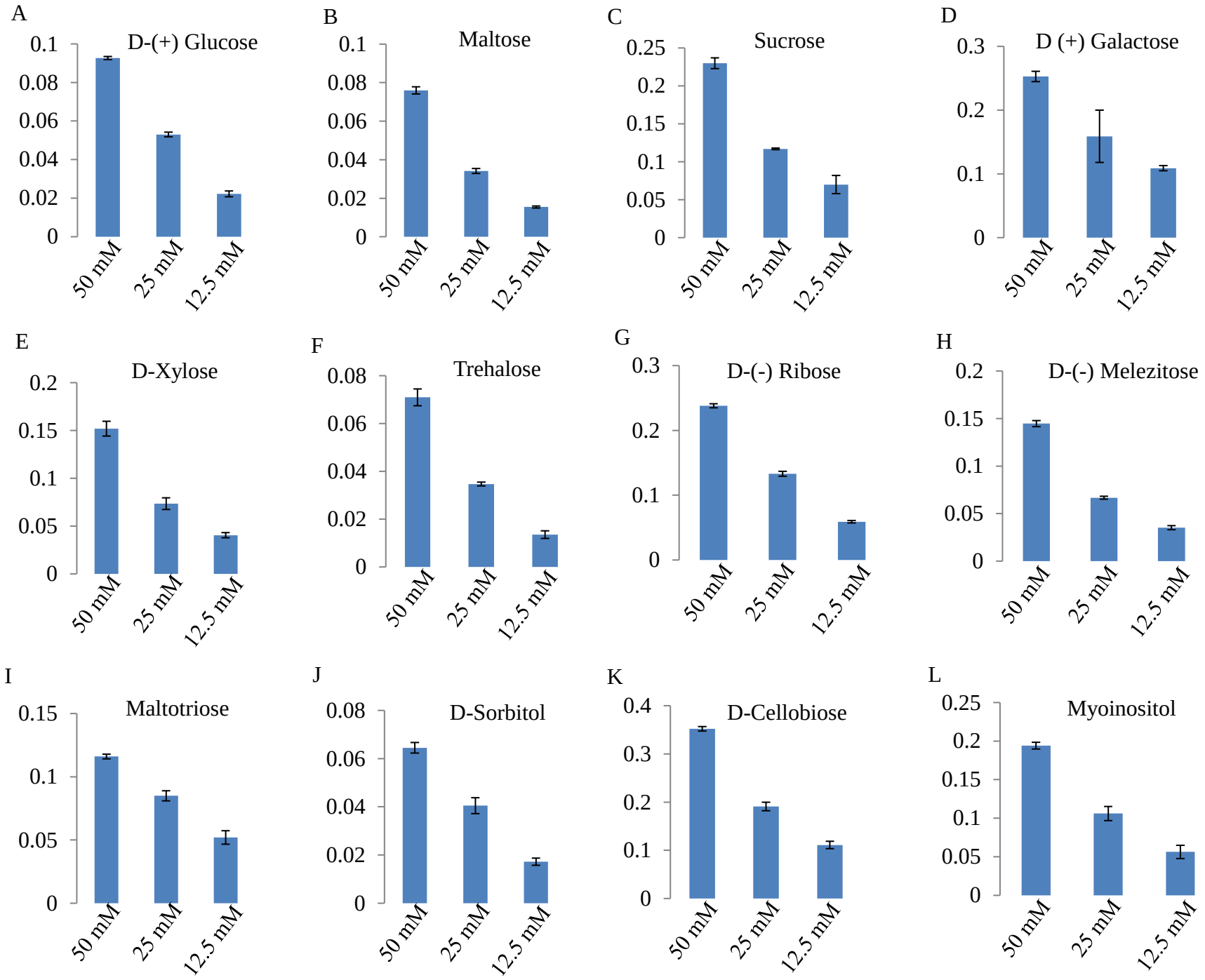
A
D-(+) Glucose
0.1
0.08
0.06
0.04
0.02
0
50 mM
25 mM
12.5 mM
B
Maltose
0.1
0.08
0.06
0.04
0.02
0
50 mM
25 mM
12.5 mM
C
Sucrose
0.25
0.2
0.15
0.1
0.05
0
50 mM
25 mM
12.5 mM
D
D (+) Galactose
0.3
0.2
0.1
0
50 mM
25 mM
12.5 mM
E
D-Xylose
0.2
0.15
0.1
0.05
0
50 mM
25 mM
12.5 mM
F
Trehalose
0.08
0.06
0.04
0.02
0
50 mM
25 mM
12.5 mM
G
D-(-) Ribose
0.3
0.2
0.1
0
50 mM
25 mM
12.5 mM
H
D-(-) Melezitose
0.2
0.15
0.1
0.05
0
50 mM
25 mM
12.5 mM
I
Maltotriose
0.15
0.1
0.05
0
50 mM
25 mM
12.5 mM
J
D-Sorbitol
0.08
0.06
0.04
0.02
0
50 mM
25 mM
12.5 mM
K
D-Cellobiose
0.4
0.3
0.2
0.1
0
50 mM
25 mM
12.5 mM
L
Myoinositol
0.25
0.2
0.15
0.1
0.05
0
50 mM
25 mM
12.5 mM